ISSCR

Nonirradiated NOD,B6.SCID $Il2r\gamma^{-/-}$ $Kit^{W41/W41}$ (NBSGW) Mice Support Multilineage Engraftment of Human Hematopoietic Cells

Brian E. McIntosh,[1] Matthew E. Brown,[2] Bret M. Duffin,[1] John P. Maufort,[1] David T. Vereide,[1,3] Igor I. Slukvin,[4,5] and James A. Thomson[1,6,7,*]

[1]Morgridge Institute for Research, Madison, WI 53715, USA
[2]Department of Surgery, University of Wisconsin, Madison, WI 53715, USA
[3]Biotechnology Center, University of Wisconsin, Madison, WI 53706, USA
[4]Wisconsin National Primate Research Center, University of Wisconsin, Madison, WI 53715, USA
[5]Department of Pathology and Laboratory Medicine, University of Wisconsin, Madison, WI 53715, USA
[6]Department of Cell and Regenerative Biology, University of Wisconsin School of Medicine and Public Health, Madison, WI 53706, USA
[7]Department of Molecular, Cellular, and Developmental Biology, University of California, Santa Barbara, Santa Barbara, CA 93106, USA
*Correspondence: jthomson@morgridgeinstitute.org
http://dx.doi.org/10.1016/j.stemcr.2014.12.005

SUMMARY

In this study, we demonstrate a newly derived mouse model that supports engraftment of human hematopoietic stem cells (HSCs) in the absence of irradiation. We cross the NOD.Cg-$Prkdc^{scid}Il2rg^{tm1Wjl}$/SzJ (NSG) strain with the C57BL/6J-Kit^{W-41J}/J (C57BL/6.Kit^{W41}) strain and engraft, without irradiation, the resulting NBSGW strain with human cord blood CD34+ cells. At 12-weeks postengraftment in NBSGW mice, we observe human cell chimerism in marrow (97% ± 0.4%), peripheral blood (61% ± 2%), and spleen (94% ± 2%) at levels observed with irradiation in NSG mice. We also detected a significant number of glycophorin-A-positive expressing cells in the developing NBSGW marrow. Further, the observed levels of human hematopoietic chimerism mimic those reported for both irradiated NSG and NSG-transgenic strains. This mouse model permits HSC engraftment while avoiding the complicating hematopoietic, gastrointestinal, and neurological side effects associated with irradiation and allows investigators without access to radiation to pursue engraftment studies with human HSCs.

INTRODUCTION

The NOD.SCID $Il2r\gamma^{-/-}$ (NSG) mouse strain dramatically improved investigators' ability to study human hematopoietic stem cell (HSC) engraftment (Rongvaux et al., 2013; Shultz et al., 2005). The NSG strain combines a series of mutations that inhibit the host's immune system by different mechanisms (Bosma et al., 1983; Cao et al., 1995; Greiner et al., 1995; Ohbo et al., 1996; Shultz et al., 1995). The NSG and other host strains require myeloablative conditioning (i.e., radiation) to achieve high levels of human chimerism (McDermott et al., 2010; Shultz et al., 2005). In addition to the effects of irradiation on the hematopoietic system that can promote engraftment (Broudy, 1997), confounding side effects of irradiation, including necrosis and apoptosis of gastrointestinal, neural, and muscle tissues, can lead to wasting, infection, and even death (Li et al., 2004; Qiu et al., 2010). Two recent studies report limited success in engrafting human HSCs into nonmyeloablated NSG hosts, but the chimerism achieved in the peripheral blood was modest (an average of 3% ± 3% and 18.3% ± 13%) (Brehm et al., 2012; Bueno et al., 2010).

Viable mutant *Kit oncogene* (*Kit*) murine strains support the engraftment of mouse hematopoietic cells without host irradiation (Wang and Bunting, 2008). The *Kit* (i.e., c-Kit, stem cell factor [SCF] receptor) encodes a type I membrane protein in the type III tyrosine kinase growth factor receptor family (Yarden and Ullrich, 1988), which is expressed on hematopoietic, melanocyte, neural, and germ cells (Mintz and Russell, 1957; Poole and Silvers, 1979; Russell, 1979). When its ligand, SCF, binds to c-Kit, it induces receptor homodimerization and signal transduction (Hsu et al., 1997). The c-Kit is required for normal hematopoiesis, and viable mutants most closely resemble aplastic anemia (Geissler et al., 1981). Mouse hosts with mutations in *Kit* thus provide a competitive advantage for WT donor cells and allow the engraftment of HSCs with reduced or no irradiation (Fleishman, 1996; Waskow et al., 2009). Until recently, these strains have been short-lifespan heterozygotes (e.g., $Kit^{+/Wv}$), causing a burden on producing experimental hosts (Cosgun et al., 2014; Waskow et al., 2009). We demonstrate that nonirradiated NBSGW mice are similar in chimerism to that achieved in irradiated NSG (irNSG) mice and that NBSGW mice also support the serial transplantation of HSCs.

RESULTS

Nonirradiated Xenograft NBSGW Mice Show Increased Chimerism in the Peripheral Blood when Compared with Non-irNSG Mice and Are Similar to Irradiated NSG Mice

We outcrossed mice homozygous for the Kit^{W41} allele with the NSG strain. The resultant F1 triple-heterozygotes
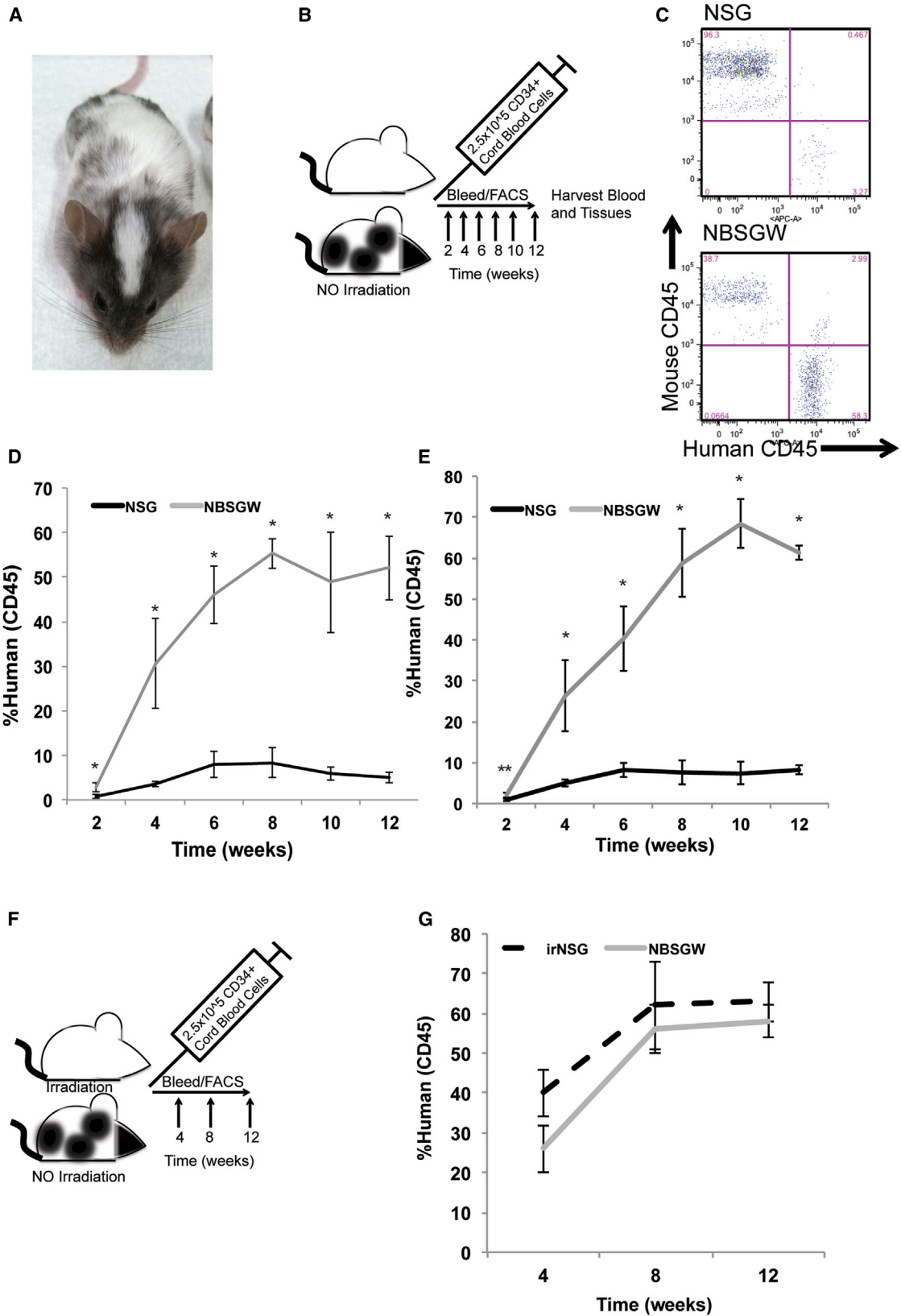
(legend on next page)

Table 1. Observed Percentages of Human CD45+ Cells at 12-Weeks Postxenograft or Serial Transplant in Hematopoietic Compartments of Nonirradiated Mice

Location	Marker (Cell)	NSG (%)	NBSGW (%)
Peripheral Blood	CD3+ (lymphoid, T cell)	3.1 ± 2.0	3.3 ± 1.5
	CD19+ (lymphoid, B cell)	46.4 ± 3.2	68.4 ± 2.9*
	CD11b+ (myeloid)	3.4 ± 1.4	2.5 ± 0.5
	CD15+ (Neut, Eos, Mono)	2.4 ± 2.2	1.4 ± 0.2
	CD66b+ (Gran)	2.5 ± 1.5	2.1 ± 0.3
Bone Marrow	CD3+ (lymphoid, T cell)	3.5 ± 0.5	5.4 ± 1.0
	CD19+ (lymphoid, B cell)	86.0 ± 2.0	89.0 ± 1.1
	CD19+IgM+ (lymphoid, B cell)	0.3 ± 0.1	0.5 ± 0.1
Spleen	CD3+ (lymphoid, T cell)	3.6 ± 1.5	3.0 ± 1.5
	CD56^{low}/+ (NKT cell)	0.8 ± 0.3	1.0 ± 0.3
Secondary Graft	CD3+ (lymphoid, T cell)	ND	0.3 ± 0.6
Peripheral Blood	CD19+ (lymphoid, B cell)	ND	87.8 ± 4.6
	CD11b+ (myeloid)	ND	8.5 ± 6.5

Error is represented by SD (n = 5, *p < 0.01). Eos, eosinophil; Gran, granulocyte; Mono, monocyte; ND, not determined; Neut, neutrophil.

(*Prkdc*, *Il2rg*, *Sirpa*, *Kit^{W41}*) were intercrossed and genotyped by Sanger sequencing for homozygotes of all four alleles (NBSGW). Nonalbino NBSGW mice displayed a Holstein coat with a prominent white stripe down the center of their head (Figure 1A). However, the NSG strain's albino coat color was inherited in 25% of the F2 progeny, making *Kit* status difficult to visually determine. To generate a strain devoid of albino animals and to allow for visual phenotyping for *Kit* status during the establishment of the strain, we selected for mice genotyping homozygous WT at the Tyrosinase allele (Shibahara et al., 1990). Albino animals were absent from future generations.

To determine whether the homozygous *Kit^{W41}* allele would enhance human hematopoietic chimerism, we intravenously injected 2.5 × 10^5 human CD34+ cord blood cells (CBCs) into the retro-orbital sinus of non-irNSG and NBSGW 8- to 10-week-old mice (Figure 1B). Every other week, peripheral blood was drawn and analyzed via flow cytometry for the presence of human and mouse blood cell surface proteins (Figure 1C). In two independent experiments (experiment 1, n = 3, Figure 1D; experiment 2, n = 5; Figure 1E) and at each independent time point, the NBSGW strain engrafted at higher levels than the NSG strain. At the 12-week time point, the average percentage of human chimerism observed in the NBSGW strain (61% ± 2%) measured 9-fold higher when compared with the parental control NSG strain (8.3% ± 1.2%; Figures 1D and 1E).

Both T cells (CD3+) and myeloid (CD11b+, CD15+, CD66b+) cells represented a similar percentage of human cells in both NSG and NBSGW hosts (Table 1). However, the percentage of B cells was significantly increased in the NBSGW strain (68.4% ± 2.9%) compared with the NSG strain (46.4% ± 3.2%, p < 0.01).

We performed a separate experiment to investigate how comparable NBSGW mice are to the field's standard model: irNSG mice (Figure 1F). As described above, we injected 2.5 × 10^5 human CD34+ CBCs into the retro-orbital sinus of the hosts and assessed the peripheral blood monthly for presence of human cells by flow cytometry. At the 12-week time point, both strains xenografted similarly indicating that genetic myeloablation may be similar to irradiating hosts (n = 3; Figure 1G).

NBSGW Mouse Marrow Contains Lymphoid, Myeloid, and Erythroid Human Cells

At 12-weeks postengraftment, the NBSGW strain had a higher percentage of human cells in the bone marrow (97% ± 0.4%) compared with the NSG strain (30% ± 9%; p < 0.01; Figures 2A and 2B). In addition, this corresponded to a higher percentage of human CD34+ in NBSGW marrow (18.6% ± 2.5%) compared with NSG marrow (6.4% ± 1.7%; Figures 2C and 2D available online). Glycophorin A (GlyA) analysis revealed a substantial presence of human erythroid cells in NBSGW marrow (26.4% ± 10.4%; Figures 2F and 2G), but not in NSG marrow (0.12% ± 0.04%). Further analysis of the hosts' peripheral blood

Figure 1. Nonirradiated NOD,B6.*Prkdc^{scid} Il2rg$^{tm1Wjl/SzJ}$ Kit$^{W41/W41}$* (NBSGW) Mice Are Similar to Their irNSG Counterparts and Exhibit High Levels of Human Chimerism in the Absence of Irradiation

(A) An NBSGW mouse.
(B) Experimental design of nonirradiation comparisons.
(C) Representative flow cytometry plots of non-irNSG and NBSGW mice 12-weeks postengraftment and analysis of mouse and human CD45.
(D and E) Biweekly monitoring of the human chimerism in the peripheral blood of non-irNSG and of NBSGW mice. Error is represented by SD (n = 3 and n = 5, *p < 0.01, **p < 0.05).
(F) Experimental design of irNSG versus nonirradiated NBSGW.
(G) Monthly monitoring comparison of the human chimerism in peripheral blood of irNSG and of nonirradiated NBSGW strains. Error is represented by SD, n = 3, comparison only, not significant.
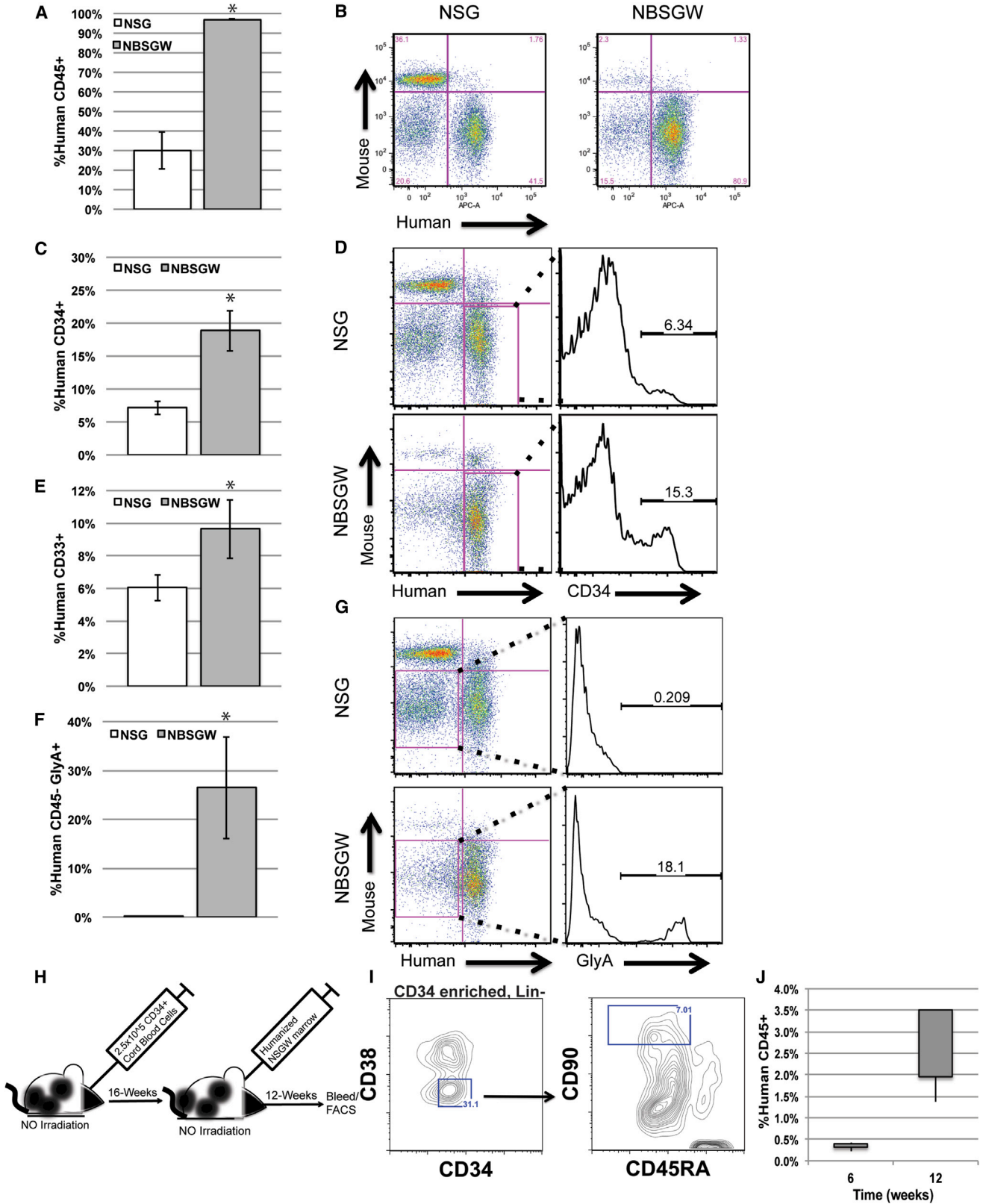
(legend on next page)

did not reveal GlyA+ cells in circulation (data not shown). Furthermore, myeloid cells were present at a higher level in NBSGW marrow (Figure 2E), whereas human T cells (CD3+) and B cells (CD19+) in the bone marrow were at similar levels in both strains (Table 1).

Serial Transplantation and Normal HSC Development Occurs in the NBSGW Strain

To demonstrate effective development of long-term reconstituting HSCs in NBSGW marrow, we performed serial transplantation of HSCs. The primary NBSGW recipient received an injection of 2.5×10^5 human CD34+ CBCs into the retro-orbital sinus (Figure 2H). At 16-weeks postxenotransplant, we assessed the primary recipient marrow for long-term reconstituting human cells by flow cytometry. We identified a population of human Lin$^-$CD34$^+$CD38$^-$CD90$^+$CD45RA$^-$ cells in murine marrow, indicating that normal hematopoietic development was occurring in the NBSGW host (Figure 2I). We performed transplants of humanized marrow to secondary recipients (n = 4) and assessed the recipients' peripheral blood for de novo produced human cells. At both 6 and 12 weeks postengraftment, we observed human cells in the peripheral blood. At 12 weeks, 2.1% ± 1.0% of the leukocytes stained positive for human CD45 (Figure 2J). This trend increased from 6 to 12 weeks, indicating an expansion of the secondary graft. In addition, we observed multilineage reconstitution of the recipient with both lymphoid and myeloid components indicating successful secondary transplantation (Table 1).

Lymphoid Organs of Humanized NBSGW Mice Reconstitute with Human Cells and Begin to Recapitulate Immunocompetent Architecture

The spleen-to-body weight ratios from nonengrafted control NBSGW and NSG mice were, on average, six times smaller compared with those from immunocompetent C57BL/6J mice (Figure 3D) and lacked white lymphocyte pulp (Figure 3F). Xenografted NBSGW spleens almost tripled in size compared with their unengrafted NBSGW counterparts (Figure 3D) and had a restored white pulp (Figure 3F). Interestingly, on average, nonengrafted NBSGW spleens are smaller than spleens of the NSG strain (Figure 3F).

At 12-weeks postinjection, 94% ± 2% of the splenocytes in NBSGW were huCD45+ compared with 55% ± 13% in NSG spleens (Figure 3A). In agreement with the flow cytometry data, αhuCD45 staining of NBSGW spleen histological sections revealed more extensive staining than those of NSG spleens (Figure 3E). We also observed increased staining of NBSGW spleen sections for both myeloid (CD11b) and dendritic cells (CD1a) compared with NSG spleens (Figure 3E). Although the level of chimerism overall was higher in the NBSGW spleen, the percentage of the human cells that were T cells, natural killer T cells, and B cells was roughly similar in both strains (Table 1; Figure 3B). Analysis of the transitional CD19+ population signified a normal B cell maturation repertoire occurring in both strains of mice. Of the huCD45+CD19+ cells, 53% ± 3% stained positively for IgM in the NSG strain compared with 61% ± 4% in the NBSGW strain (Figure 3C; p = 0.013).

Thymuses were obtained from nonirradiated NBSGW mice (seven of eight), but we were unsuccessful in definitively identifying like thymic tissue in non-irNSG mice (zero of eight). This made a technical comparison challenging. However, we evaluated the NBSGW for both human MHCII and human CD3. The analysis indicated that thymuses were low in staining for human MHCII, yet CD3 staining was found to be in abundance within the tissue (Figure 3G). Further, analysis indicated a lack of thymic structure with a very disorganized cortex and nonexistent medulla.

DISCUSSION

In this study, we generated mice homozygous for *Prkdc*^{scid}, *Il2rγ*$^{-/-}$, *Kit*^{W41}, and NOD *Sirpa* alleles and showed that

---

Figure 2. Xenotransplanted Nonirradiated NBSGW Mice Exhibit Increased Humanization in the Marrow and Are Conducive to Serial Transplantation

(A) The percentage of observed human CD45+ leukocytes in the bone marrow of non-irNSG (white) and NBSGW (gray) mice at 12-weeks postengraftment.

(B) Representative mouse CD45 versus human CD45 12-week flow cytometry plot comparison between non-irNSG and NBSGW mice.

(C) The observed percentages of human CD34+ cells in the human CD45+ fraction of the mouse marrow (NSG, white; NBSGW, gray).

(D) Representative flow cytometry analysis plot comparison between non-irNSG and NBSGW mice.

(E) The observed percentages of human CD33+ cells observed in the human CD45+ fraction of the mouse marrow (NSG, white; NBSGW, gray).

(F) The observed percentage of human GlyA+ cells observed in the mouse marrow (NSG, white; NBSGW, gray).

(G) Representative flow cytometry analysis plot comparison between non-irNSG and NBSGW mice.

(H) Experimental design of nonirradiation NBSGW serial transplantation.

(I) Representative flow cytometry analysis of CD34 enriched Lin−CD34+CD38−CD90+CD45RA− cells isolated from the NBSGW marrow at 16 weeks.

(J) Observed human chimerism at both 6 and 12 weeks in secondary NBSGW recipients. (Error is represented by SD, *p < 0.01).
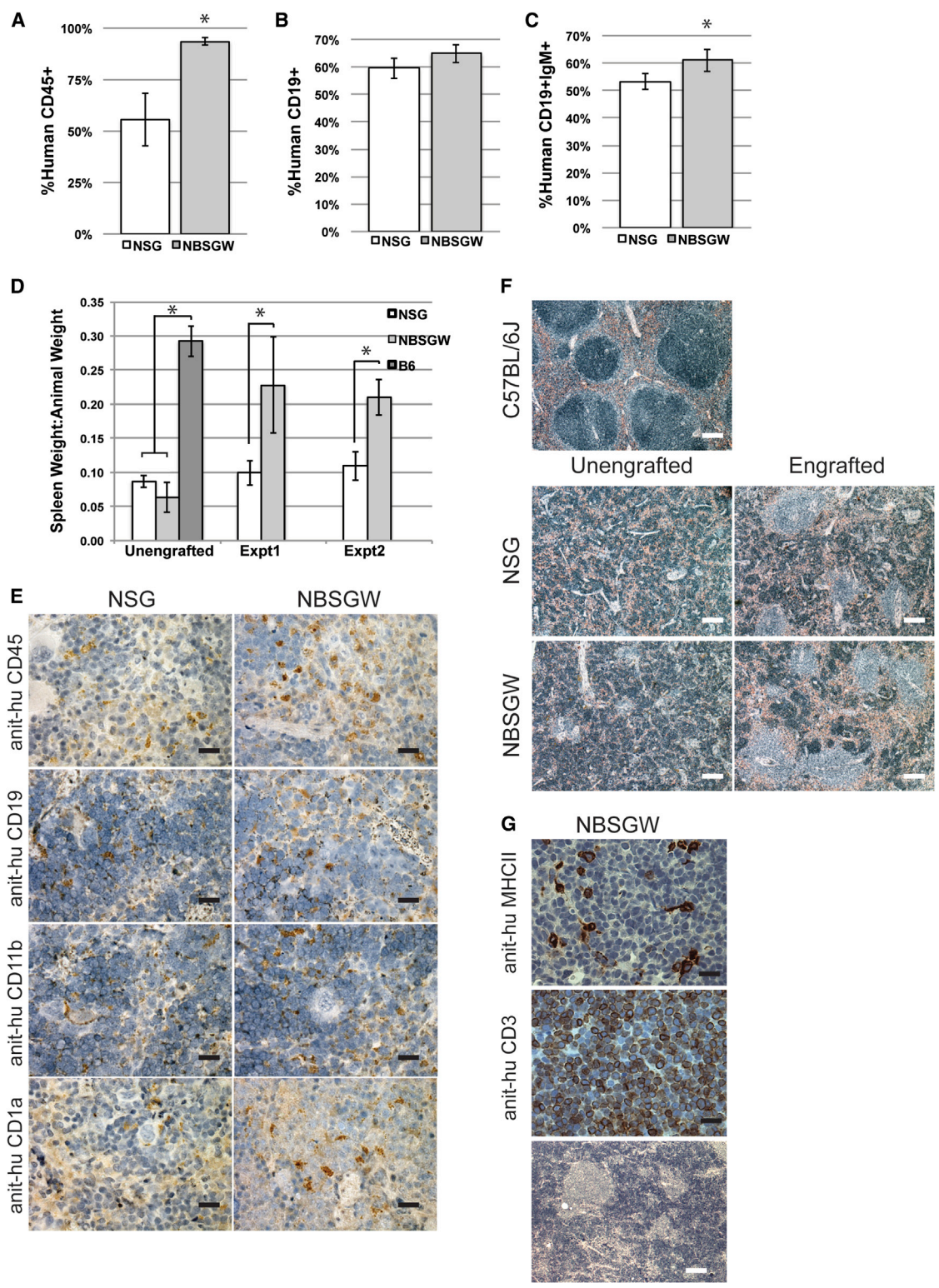
Figure 3. Human Chimerism, Lineage Development and Gross Pathology Observed in Lymphoid Organs of Non-irNSG (White) and NBSGW (Gray) Mice at 12-Weeks Postengraftment

(A) The percentage of human CD45+ splenocytes (non-irNSG [white] and NBSGW [gray]).

(B and C) The percentage of human (B) CD19+ cells and (C) CD19+IgM+ cells observed in the human CD45+ fraction.

(legend continued on next page)

the resultant NBSGW model supports robust levels of humanization in peripheral blood, bone marrow, and spleen in the absence of irradiation. The observed levels of de novo derived human HSCs in NBSGW mice are significantly higher than the values previously reported for unconditioned NSG or NSG-transgenic mice (Brehm et al., 2012; Bueno et al., 2010). In our studies, the unconditioned NBSGW strain supported levels of human chimerism in peripheral blood that was 9-fold higher (average 61% versus 8.3%) compared with the unconditioned NSG strain. Furthermore, these levels are equivalent to those recently reported in multiple irradiated $Rag2^{-/-}$ $Il2\gamma^{-/-}$ mice possessing humanized loci for TPO, $CSF1$, $IL3$, and $CSF2$ in which hematopoietic development is enhanced (Rongvaux et al., 2011, 2014). We further demonstrate, through serial transplantation, robust normal development of human HSCs in NBSGW marrow and the developing HSCs ability to repopulate a secondary recipient. To our knowledge, $Kit^{W41/41}$ mutants when combined with NSG mice yield the highest level of human hematopoietic chimerism obtained in any mouse strain without conditioning by ionizing radiation.

While this manuscript was in review, four Kit mutant strains on either the BALB/c $RAG1^{-/-}$ (BRg $Kit^{Wv/Wv}$, BRgWv) or NSG (NSG $Kit^{Wv/Wv}$, NSGWv; NSGWv/+, and NSGW41) backgrounds were described (Cosgun et al., 2014). These strains are similar to the NBSGW model exhibiting comparable humanization potential in the absence of irradiation. Both BALB/c and NOD immunodeficient-based strains support varied types of humanization. However, NOD background strains have higher humanization potential (Brehm et al., 2010) primarily resulting from polymorphisms in the $Sirpa$ gene that prevents the NOD macrophages from engulfing human cells (Takenaka et al., 2007). Hence, the Kit mutant strains NBSGW, NSGWv, NSGWv/+, and NSGW41 are better suited recipients when compared with the BRgWv strain. Homozygous Kit^{Wv} NSG mice have a low life expectancy, making the NSGWv/+ the more useful of the two for long-term experiments (Cosgun et al., 2014). However, genotyping to identify suitable NSGWv/+ recipients among litters is time consuming.

Our goal was to generate a viable homozygous strain that would engraft with high efficiency without irradiation. Based on previously reported Kit mutant phenotypes (Geissler et al., 1981), we hypothesized that the Kit^{W41} could be maintained as a homozygous line when crossed with the NSG, and the contribution of the NSG strain would boost the efficiency of humanization in the absence of irradiation. While the NBSGW is a mixed NOD and C57BL/6J background, the Cosgun strain is a congenic NOD also incorporating a homozygous Kit^{W41} allele. A direct comparison of engraftment results between the two strains is currently difficult due to differences in experimental approaches (e.g., cell numbers and sources) and reported postengraftment end points (e.g., 12 weeks versus up to 40 weeks). However, the highest levels of engraftment in the absence of irradiation were observed in homozygous Kit^{W41} immunocompromised mice in both studies, potentially indicating that a mixed background is inconsequential given the correct genetic elements. Based on these arguments, either the NBSGW or the NSGW41 strains are of choice over their contemporary strains in the absence of irradiation and may prove as a widely enabling resource.

In addition to the increased human chimerism in the blood, we observed a significantly greater percentage of de novo human erythroid cells in the marrow of NBSGW mice (average 26.0% versus 0.1%). These levels are ∼5–12 times higher on average than previous reports with irNSG mice (Hayakawa et al., 2010; McDermott et al., 2010). However, our analysis of peripheral blood for GlyA+ cells did not indicate we had achieved circulating human erythrocytes, suggesting that the current mouse model still lacks signals to complete human erythrogenesis.

The NBSGW mice exhibit a high degree of human chimerism, albeit a bias in differentiation of the engrafted human hematopoietic cells remains. In normal human peripheral blood, granulocytes, T cells, and B cells are present at 53%, 20%, and 33%, respectively (Rongvaux et al., 2013), but within our study, they are present at 2.5%, 3.3%, and 68%, respectively. These biases are comparable to those previously observed in other mouse xenograft models (Brehm et al., 2010; Cosgun et al., 2014; McDermott

(D) The ratio of spleen:mouse weight in basal state (unengrafted, n = 4) and two xenograft experiments (C57BL/6J; dark gray, experiment 1, n = 5; experiment 2, n = 3). Error is represented by SD (*p < 0.01).
(E) Representative photomicrographs of sectioned spleens of non-irNSG and NBSGW mice at 12-weeks postengraftment (based on flow cytometry data). Spleens were stained with anti-human CD45 (splenocyte), anti-human CD19 (B cell), anti-human CD11b (myeloid), and anti-human CD1a (dendritic) and were counterstained with hematoxylin (blue; the black scale bar is 20 μm).
(F) Photomicrographs of hematoxylin (blue) and eosin (red) stained spleens from nonirradiated, nonengrafted mouse strains (left), and nonirradiated humanized mice at 12 weeks (right; white scale bar represents 400 μm).
(G) Representative photomicrographs of sectioned thymus from non-irradiated NBSGW mice at 12-weeks postengraftment; anti-human MHCII (top), anti-human CD3 (middle), and hematoxylin (blue) and eosin (red) stained (bottom; white scale bar represents 400 μm; black scale bar represents 20 μm).

et al., 2010) and suggest that deficiencies exist in species cross-reactivity of signaling molecules supporting typical human hematopoietic cell distributions (Rongvaux et al., 2013). Additional genetic modifications to NBSGW mice are possible with the aim of eliminating these biases. Such modifications might include replacing growth factors or matrix molecules that poorly cross-react between mouse and human species. A number of recently described strains, when crossed with NBSGW, might further improve the differentiation of human HSCs (Billerbeck et al., 2011; Brehm et al., 2012; Rongvaux et al., 2014).

Although the main focus of our study was to grade the relative efficiency of human HSC engraftment in a nonirradiated mouse model, the lack of T cell production in NBSGW, NSGW41 and NSG warrants further discussion. All three strains support the production of a limited number of T cells (Cosgun et al., 2014). This may be partially due to a relatively thin thymic membrane and to the documented poor thymic microenvironment (McDermott et al., 2010; Shultz et al., 2005) for all strains. Furthermore, in this study, we measured engraftment at 12 weeks, while T cell development is building and not yet plateaued (Hiramatsu et al., 2003). However, the data and reports indicate that T cell production is elevated in the homozygous Kit^{W41} strains in comparison to others (Cosgun et al., 2014). In sum, these facts create an opportunity to improve humanized murine models via the improvement of thymic function. Pluripotent stem cell (PSC) technology offers one potential route to re-establish human thymic function in humanized mouse models (Takahashi et al., 2007; Yu et al., 2007). For example, two recent publications report the correction of a developmental T cell deficiency in immunocompromised mice (Parent et al., 2013; Sun et al., 2013). After differentiating human embryonic stem cells to a thymic epithelial progenitor cell type and grafting these cells into mice, the authors produced human thymic structures capable of further development and education of both mouse and human T cells in vivo (Parent et al., 2013; Sun et al., 2013). Thus, further refinements of PSC technology may afford even better opportunities to study allogeneic and autologous human HSC transplantation in the in vivo mouse environment.

A variety of suitable murine xenograft models are currently used in hematopoietic research, yet these animals require conditioning prior to experimentation. Given the increasingly restricted access to radiation sources, NBSGW mice are broadly enabling, allowing laboratories without access to radiation to accelerate human hematopoietic research. The NBSGW model and other homozygous mice possessing the Kit^{W41} allele are significant steps toward providing a standardized framework and an improved understanding of human HSC biology.

EXPERIMENTAL PROCEDURES

Animals

The C57BL/6.Kit^{W41} and the NSG strains were obtained from the Jackson Laboratory (Geissler et al., 1981; Shultz et al., 2005). The NSG mouse strain was intercrossed with mice homozygous for the Kit^{W41} allele and the resultant progeny bred (NBSGW) to homozygosity (for $Prkdc^{scid}$, $Il2rg^-$, Kit^{W41}, $Sirpa^{NOD}$, Tyr^A). The NBSGW mice (JAX Stock No. 026622) were maintained as homozygotes. All breeding males were retired after 1 year of age. See Supplemental Experimental Procedures for oligos and allelic determination. The University of Wisconsin Medical School's Animal Care and Use Committee authorized all experiments.

Human Cell Engraftment

Frozen human CD34+ CBCs (AllCells) were thawed per manufacturer's recommendation and incubated overnight in serum-free media (STEMCCELL Technologies) supplemented with human SCF (100 ng/ml; Peprotech). The next morning, live cells were counted using a hemocytometer and trypan blue. Cells were suspended at 1.25×10^6 per ml in a 10 mM HEPES buffered Hank's balanced salt solution (Life Technologies). Eight- to 10-week-old male mice anesthetized with isoflurane were injected retro-orbitally with 200 μl cell suspension. Serial transplants were conducted using bone marrow cells recovered from mice engrafted with CD34+ CBCs. Irradiation of NSG mice was carried out using an X-RAD 320ix irradiator (Precision X-Ray) at 250 RAD.

Human Xenograft Analysis

A 50 μl blood sample was drawn into heparin-coated capillary tubes from the retro-orbital sinus and processed for flow cytometric analysis. At 12-weeks postengraftment, tissues were removed for analysis. Multipotent progenitor analysis was performed as previously described (Majeti et al., 2007). See the Supplemental Experimental Procedures for processing and antibodies. Flow cytometry was performed on a BD AriaIII and analyzed using FlowJo Version 9.5.2 (Tree Star).

Statistics

A two-sided Wilcoxon rank-sum test was performed using the statistical software program MStat 5.5 (http://mcardle.oncology.wisc.edu/mstat/) to determine the statistical significance between experimental groups; n = number of experimental mice per group.

Histology and Immunohistochemistry

Tissues were fixed in 10% neutral-buffered formalin, processed at the University of Wisconsin Veterinary School Histology Lab, and developed as previously described (Maufort et al., 2010). Slides were analyzed on a Zeiss AxioScope-A1 with EC Plan-NeoFluar −5 × or −40×/0.75 objectives, and images acquired using a Q-Imaging Micropublisher 3.3RTV camera and iVision v.4.5.0.

SUPPLEMENTAL INFORMATION

Supplemental Information includes Supplemental Experimental Procedures and one table and can be found with this article online at http://dx.doi.org/10.1016/j.stemcr.2014.12.005.

REFERENCES

Billerbeck, E., Barry, W.T., Mu, K., Dorner, M., Rice, C.M., and Ploss, A. (2011). Development of human CD4+FoxP3+ regulatory T cells in human stem cell factor-, granulocyte-macrophage colony-stimulating factor-, and interleukin-3-expressing NOD-SCID IL2Rγ (null) humanized mice. Blood *117*, 3076–3086.

Bosma, G.C., Custer, R.P., and Bosma, M.J. (1983). A severe combined immunodeficiency mutation in the mouse. Nature *301*, 527–530.

Brehm, M.A., Cuthbert, A., Yang, C., Miller, D.M., DiIorio, P., Laning, J., Burzenski, L., Gott, B., Foreman, O., Kavirayani, A., et al. (2010). Parameters for establishing humanized mouse models to study human immunity: analysis of human hematopoietic stem cell engraftment in three immunodeficient strains of mice bearing the IL2rgamma(null) mutation. Clin. Immunol. *135*, 84–98.

Brehm, M.A., Racki, W.J., Leif, J., Burzenski, L., Hosur, V., Wetmore, A., Gott, B., Herlihy, M., Ignotz, R., Dunn, R., et al. (2012). Engraftment of human HSCs in nonirradiated newborn NOD-scid IL2rγ null mice is enhanced by transgenic expression of membrane-bound human SCF. Blood *119*, 2778–2788.

Broudy, V.C. (1997). Stem cell factor and hematopoiesis. Blood *90*, 1345–1364.

Bueno, C., Montes, R., de la Cueva, T., Gutierrez-Aránda, I., and Menendez, P. (2010). Intra-bone marrow transplantation of human CD34(+) cells into NOD/LtSz-scid IL-2rgamma(null) mice permits multilineage engraftment without previous irradiation. Cytotherapy *12*, 45–49.

Cao, X., Shores, E.W., Hu-Li, J., Anver, M.R., Kelsall, B.L., Russell, S.M., Drago, J., Noguchi, M., Grinberg, A., Bloom, E.T., et al.

(1995). Defective lymphoid development in mice lacking expression of the common cytokine receptor gamma chain. Immunity *2*, 223–238.

Cosgun, K.N., Rahmig, S., Mende, N., Reinke, S., Hauber, I., Schäfer, C., Petzold, A., Weisbach, H., Heidkamp, G., Purbojo, A., et al. (2014). Kit regulates HSC engraftment across the human-mouse species barrier. Cell Stem Cell *15*, 227–238.

Fleishman, R.A. (1996). Engraftment of W/c-kit mutant mice is determined by stem cell competition, not by increased marrow 'space'. Exp. Hematol. *24*, 209–213.

Geissler, E.N., McFarland, E.C., and Russell, E.S. (1981). Analysis of pleiotropism at the dominant white-spotting (W) locus of the house mouse: a description of ten new W alleles. Genetics *97*, 337–361.

Greiner, D.L., Shultz, L.D., Yates, J., Appel, M.C., Perdrizet, G., Hesselton, R.M., Schweitzer, I., Beamer, W.G., Shultz, K.L., Pelsue, S.C., et al. (1995). Improved engraftment of human spleen cells in NOD/LtSz-scid/scid mice as compared with C.B-17-scid/scid mice. Am. J. Pathol. *146*, 888–902.

Hayakawa, J., Hsieh, M.M., Anderson, D.E., Phang, O., Uchida, N., Washington, K., and Tisdale, J.F. (2010). The assessment of human erythroid output in NOD/SCID mice reconstituted with human hematopoietic stem cells. Cell Transplant. *19*, 1465–1473.

Hiramatsu, H., Nishikomori, R., Heike, T., Ito, M., Kobayashi, K., Katamura, K., and Nakahata, T. (2003). Complete reconstitution of human lymphocytes from cord blood CD34+ cells using the NOD/SCID/gammacnull mice model. Blood *102*, 873–880.

Hsu, Y.R., Wu, G.M., Mendiaz, E.A., Syed, R., Wypych, J., Toso, R., Mann, M.B., Boone, T.C., Narhi, L.O., Lu, H.S., and Langley, K.E. (1997). The majority of stem cell factor exists as monomer under physiological conditions. Implications for dimerization mediating biological activity. J. Biol. Chem. *272*, 6406–6415.

Li, Y.Q., Chen, P., Jain, V., Reilly, R.M., and Wong, C.S. (2004). Early radiation-induced endothelial cell loss and blood-spinal cord barrier breakdown in the rat spinal cord. Radiat. Res. *161*, 143–152.

Majeti, R., Park, C.Y., and Weissman, I.L. (2007). Identification of a hierarchy of multipotent hematopoietic progenitors in human cord blood. Cell Stem Cell *1*, 635–645.

Maufort, J.P., Shai, A., Pitot, H.C., and Lambert, P.F. (2010). A role for HPV16 E5 in cervical carcinogenesis. Cancer Res. *70*, 2924–2931.

McDermott, S.P., Eppert, K., Lechman, E.R., Doedens, M., and Dick, J.E. (2010). Comparison of human cord blood engraftment between immunocompromised mouse strains. Blood *116*, 193–200.

Mintz, B., and Russell, E.S. (1957). Gene-induced embryological modifications of primordial germ cells in the mouse. J. Exp. Zool. *134*, 207–237.

Ohbo, K., Suda, T., Hashiyama, M., Mantani, A., Ikebe, M., Miyakawa, K., Moriyama, M., Nakamura, M., Katsuki, M., Takahashi, K., et al. (1996). Modulation of hematopoiesis in mice with a truncated mutant of the interleukin-2 receptor gamma chain. Blood *87*, 956–967.

Parent, A.V., Russ, H.A., Khan, I.S., LaFlam, T.N., Metzger, T.C., Anderson, M.S., and Hebrok, M. (2013). Generation of functional

thymic epithelium from human embryonic stem cells that supports host T cell development. Cell Stem Cell *13*, 219–229.

Poole, T.W., and Silvers, W.K. (1979). Capacity of adult steel (Sl/Sld) and dominant spotting (W/Wv) mouse skin to support melanogenesis. Dev. Biol. *72*, 398–400.

Qiu, W., Leibowitz, B., Zhang, L., and Yu, J. (2010). Growth factors protect intestinal stem cells from radiation-induced apoptosis by suppressing PUMA through the PI3K/AKT/p53 axis. Oncogene *29*, 1622–1632.

Rongvaux, A., Willinger, T., Takizawa, H., Rathinam, C., Auerbach, W., Murphy, A.J., Valenzuela, D.M., Yancopoulos, G.D., Eynon, E.E., Stevens, S., et al. (2011). Human thrombopoietin knockin mice efficiently support human hematopoiesis in vivo. Proc. Natl. Acad. Sci. USA *108*, 2378–2383.

Rongvaux, A., Takizawa, H., Strowig, T., Willinger, T., Eynon, E.E., Flavell, R.A., and Manz, M.G. (2013). Human hemato-lymphoid system mice: current use and future potential for medicine. Annu. Rev. Immunol. *31*, 635–674.

Rongvaux, A., Willinger, T., Martinek, J., Strowig, T., Gearty, S.V., Teichmann, L.L., Saito, Y., Marches, F., Halene, S., Palucka, A.K., et al. (2014). Development and function of human innate immune cells in a humanized mouse model. Nat. Biotechnol. *32*, 364–372.

Russell, E.S. (1979). Hereditary anemias of the mouse: a review for geneticists. Adv. Genet. *20*, 357–459.

Shibahara, S., Okinaga, S., Tomita, Y., Takeda, A., Yamamoto, H., Sato, M., and Takeuchi, T. (1990). A point mutation in the tyrosinase gene of BALB/c albino mouse causing the cysteine—serine substitution at position 85. Eur. J. Biochem. *189*, 455–461.

Shultz, L.D., Schweitzer, P.A., Christianson, S.W., Gott, B., Schweitzer, I.B., Tennent, B., McKenna, S., Mobraaten, L., Rajan, T.V., Greiner, D.L., et al. (1995). Multiple defects in innate and adaptive immunologic function in NOD/LtSz-scid mice. J. Immunol. *154*, 180–191.

Shultz, L.D., Lyons, B.L., Burzenski, L.M., Gott, B., Chen, X., Chaleff, S., Kotb, M., Gillies, S.D., King, M., Mangada, J., et al. (2005). Human lymphoid and myeloid cell development in NOD/LtSz-scid IL2R gamma null mice engrafted with mobilized human hemopoietic stem cells. J. Immunol. *174*, 6477–6489.

Sun, X., Xu, J., Lu, H., Liu, W., Miao, Z., Sui, X., Liu, H., Su, L., Du, W., He, Q., et al. (2013). Directed differentiation of human embryonic stem cells into thymic epithelial progenitor-like cells reconstitutes the thymic microenvironment in vivo. Cell Stem Cell *13*, 230–236.

Takahashi, K., Tanabe, K., Ohnuki, M., Narita, M., Ichisaka, T., Tomoda, K., and Yamanaka, S. (2007). Induction of pluripotent stem cells from adult human fibroblasts by defined factors. Cell *131*, 861–872.

Takenaka, K., Prasolava, T.K., Wang, J.C., Mortin-Toth, S.M., Khalouei, S., Gan, O.I., Dick, J.E., and Danska, J.S. (2007). Polymorphism in Sirpa modulates engraftment of human hematopoietic stem cells. Nat. Immunol. *8*, 1313–1323.

Wang, Z., and Bunting, K.D. (2008). Hematopoietic stem cell transplant into non-myeloablated W/Wv mice to detect steady-state engraftment defects. Methods Mol. Biol. *430*, 171–181.

Waskow, C., Madan, V., Bartels, S., Costa, C., Blasig, R., and Rodewald, H.R. (2009). Hematopoietic stem cell transplantation without irradiation. Nat. Methods *6*, 267–269.

Yarden, Y., and Ullrich, A. (1988). Growth factor receptor tyrosine kinases. Annu. Rev. Biochem. *57*, 443–478.

Yu, J., Vodyanik, M.A., Smuga-Otto, K., Antosiewicz-Bourget, J., Frane, J.L., Tian, S., Nie, J., Jonsdottir, G.A., Ruotti, V., Stewart, R., et al. (2007). Induced pluripotent stem cell lines derived from human somatic cells. Science *318*, 1917–1920.